Pergamon

Journal of Structural Geology, Vol. 19, Nos 3–4, pp. 383 to 396, 1997

0191–8141/97 $17.00+0.00

PII: S0191–8141(96)00112–5

Growth of Wheeler Ridge anticline, California: geomorphic evidence for fault-bend folding behaviour during earthquakes

KARL MUELLER* and JOHN SUPPE

Department of Geological and Geophysical Sciences, Princeton University, Princeton, NJ 08544, U.S.A.

(*Received* 1 *February* 1996; *accepted in revised form* 13 *November* 1996)

Abstract—Unique landforms, which we term fold-growth terraces and alluvial fan ridges, are interpreted to be produced by kink-band migration of the front limb of Wheeler Ridge anticline, an active fault-bend fold in the southern San Joaquin Valley. Based on a folding-related model, these features form by onlap of alluvium across an active axial surface along the tip of a thrust-wedge structure. Alluvial fan ridges record the sense of slip on the underlying blind thrust, which is composed of both thrust and left-lateral components. Our model predicts formation of fold-growth terraces by upward propagation of an active axial surface through onlapped alluvium during a folding 'event' to produce a prism of translated but otherwise undeformed sediment. Alternative hypotheses for the terraces include flexural slip faulting, solifluction and erosive processes. The width of fold limb between adjacent terraces is equivalent to fault displacement at depth, which we interpret to be related to slip caused by earthquakes on the underlying blind thrust. Earthquake magnitudes derived from the terraces are much larger than expected for the length of the active fold and thrust belt, and may indicate a kinematic link with the San Andreas fault that drives shortening in the region.

INTRODUCTION

Fault-bend folds grow in response to slip past bends in faults and develop in many tectonic environments, including fold and thrust belts (Suppe, 1983; Wilkerson *et al.*, 1991), extensional terranes (Xiao and Suppe, 1992) and along transpressive strike-slip faults (Medwedeff, 1989; Shaw *et al.*, 1992). In active thrust belts, these folds are often the only indication of potentially seismogenic blind thrusts (Stein and King, 1984; Stein and Yeats, 1989; Shaw and Suppe, 1995). Although geometric relationships between folding and faulting have been recognized for over 60 years (Rich, 1934), rapid, episodic strain which acts to build fault-bend folds during earthquake-related slip on active faults has only begun to be documented (Yielding *et al.*, 1981; Klinger and Rockwell, 1989; Treiman, 1995; Kelson *et al.*, 1996).

Fault-bend folds that develop in response to episodic, earthquake-related movement along underlying blind faults form by a number of deformation mechanisms. Fold limbs which grow by movement of hangingwall strata from flatter fault surfaces upward onto the base of thrust ramps, or above wedge tips, can exhibit bed thickening. Bed thickening is accommodated by small displacement thrust faults which cross-cut bedding as evidenced in a synclinal bend interpreted to form above a wedge tip that was uplifted during the **M**6.8 Northridge earthquake (Treiman, 1995). Flexural slip faulting, or bedding-parallel shear is also an important process in these geometric settings and has been documented to occur during the Superstition Hills earthquake by Klinger and Rockwell (1989), the Northridge earthquake (Treiman, 1995) and in the cores of Wheeler Ridge (Medwedeff, 1992) and the Ventura Avenue anticline (Rockwell *et al.*, 1988). Evidence for the development of a narrow kink-band formed during a thrust-type earthquake has also been documented by Treiman (1995) for the Northridge event.

Extensional faulting is common on fold limbs that form by collapse of hangingwall strata onto the top of ramps, or convex upward fault bends. Examples of this process have been documented for historic thrust-type earthquakes in Algeria (Yielding *et al.*, 1981), Armenia (Philip *et al.*, 1992), and in the eastern United States along the Reelfoot Scarp, a fault-bend fold uplifted in a great earthquake in 1812 (Kelson *et al.*, 1996). These highly destructive thrust-type earthquakes illustrate the societal importance for better understanding of how fault-bend folds grow during slip above otherwise inaccessible blind faults in active orogenic belts. As a case in point, the 1994 **M**6.8 Northridge earthquake in Los Angeles caused over 70 deaths and cost 10 billion dollars in property damage in the second most costly disaster in U.S. history.

We present new models, maps, trench logs and topographic profiles of folded geomorphic surfaces and syntectonic growth sediments deposited above Wheeler Ridge anticline, a fault-bend fold formed at the leading edge of the active Transverse Ranges fold and thrust belt in central California (Fig. 1; Namson and Davis, 1988) The eastern portion of Wheeler Ridge is ideal for our analysis because the subsurface structure there has been tightly constrained by Medwedeff (1992) using abundant oilfield well data. The rate of uplift of Wheeler Ridge is more rapid than burial by syntectonic alluvial deposits (Medwedeff, 1992), providing an oportunity to document folding processes that have acted to build it for the

*Present address: Department of Geological Sciences, University of Colorado, Boulder, CO 80309, U.S.A.

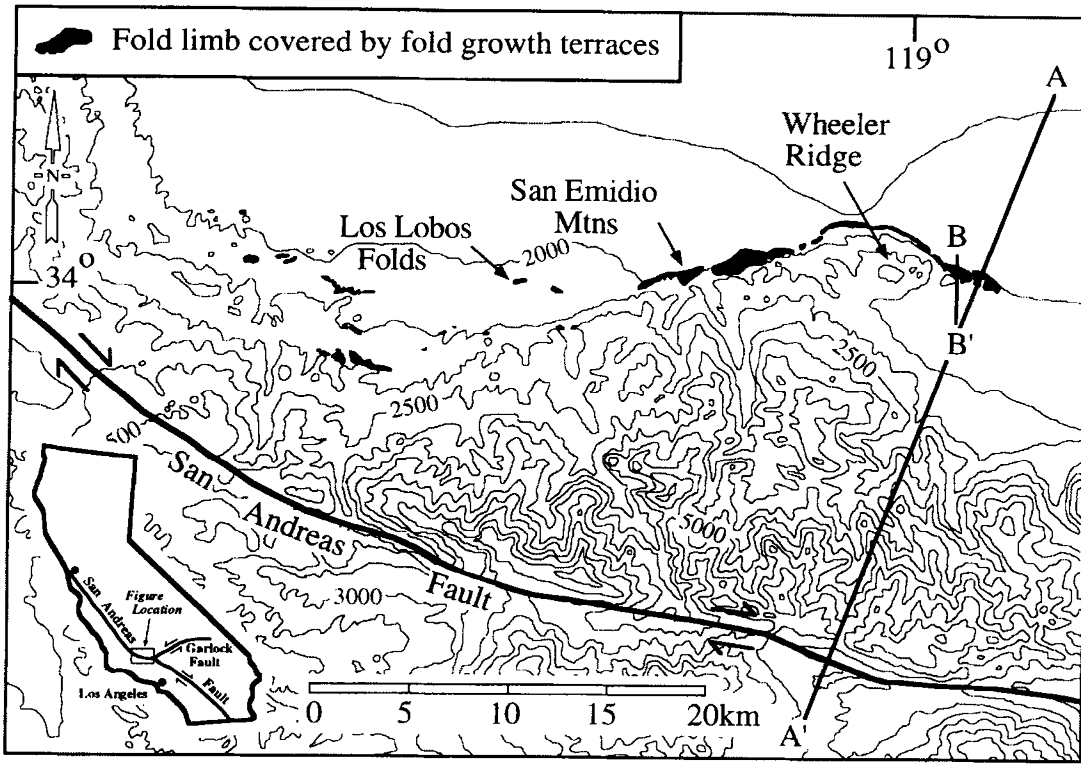

Fig. 1. Topographic map of the northern Transverse Ranges and southern San Joaquin Valley marked with locations of fold growth terraces on the northern limbs of active folds such as Wheeler Ridge anticline, the San Emigdio Mountains, Los Lobos and other structures. Note the NW end of the 'Big Bend', a major restraining bend in the strike-slip San Andreas fault, which corresponds with the western end of the active fold trend. Our study is focused on Wheeler Ridge where abundant oilfield data are available. The triangular area of high relief located between the active folds and the San Andreas fault is formed in response to shortening across a thin-skinned fold and thrust belt, developed in the upper 5 km of the crust. Contour interval equals 500 feet.

last 125 Ka. This allows us to model and document landforms developed on the front limb of Wheeler Ridge, which record rates and styles of forward propagation. The geomorphology of Wheeler Ridge has also been broadly studied by Zepeda *et al.* (1996) who developed a chronology for the age of folded alluvial deposits and by Mueller and Talling (1997) who evaluated the relationship of tear faults to lateral propagation of the fold.

Although numerous studies have illustrated the depositional and geomorphic response to folding caused by progressive limb rotation (Rockwell *et al.*, 1988; Burbank and Verges, 1994; Hardy and Poblet, 1994), less is known about the geomorphic response to folds that are known to grow by kink-band migration. We have therefore integrated existing subsurface structural mapping by Medwedeff (1992) from an active fault-bend fold with new modeling and mapping of unique geomorphic landforms which we believe to develop by kink-band migration.

This is important for research in both active tectonics and seismic risk analysis where workers are challenged with predicting the geometry of otherwise inaccessible and/or poorly imaged blind thrusts. It also allows comparison of small-scale structures formed on active folds with ancient examples where timing is poorly constrained (i.e. the 'snapshot in time' is not afforded the observer). Our hope is that this work will shed light on often contradictory models of structural growth in ancient fold and thrust belts which do not have the added geomorphic information contained in active orogens. The key focus of our work is therefore to document landforms which may have formed by active kink-band migration of fold limbs in subaerial depositional environments.

REGIONAL SETTING

Wheeler Ridge anticline lies at the eastern end of a trend of active folds (Fig. 1) which define the northern edge of the Transverse Ranges of south-central California (Seaver, 1986; Namson and Davis, 1988; Laduzinsky, 1989; Medwedeff, 1992; Burbank and Verges, 1994; Zepeda *et al.*, 1996). This fold belt has formed in response to crustal shortening across a broad restraining bend in the right-lateral San Andreas fault. The leading edge of the fold and thrust belt corresponds closely with the abrupt onset of a major restraining bend in the San Andreas, which together form the southwestern corner of the San Joaquin Valley (Fig. 1).

Structurally high parts of the belt are characterized by

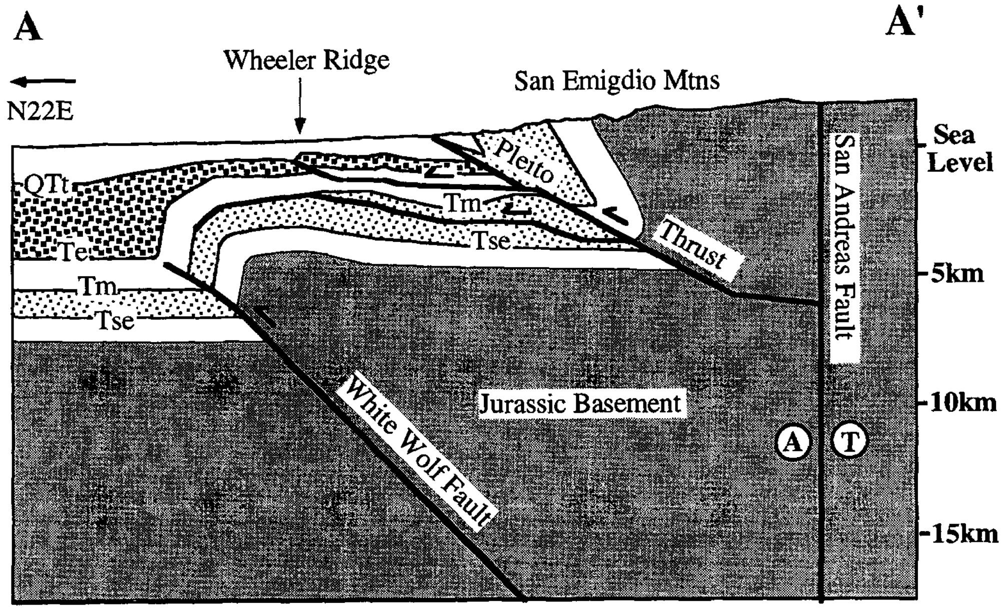

Fig. 2. Regional cross section A–A′, modified from work by Medwedeff (1988) which extends SSW from the southern San Joaquin Valley across a fold and thrust belt developed in the upper 7 km of the seismogenic crust in response to shortening across a restraining bend in the San Andreas fault. Note the location of Wheeler Ridge, the frontal active fold in the thin-skinned part of the belt. It overlies the White Wolf fault, a large displacement, high-angle reverse fault which offsets basement. Its location is well constrained by the M7.6 1952 Arvin–Tehachepi earthquake and aftershock sequence which originated beneath Wheeler Ridge at about 17 km depth. The location of the cross-section is shown on Fig. 1. Stratigraphic units include the tops of the Tulare Fm (QTt), the Echegoin Fm (Te), the Monterey Fm (Tm), the San Emigdio Fm (Tse), and the top of Jurassic basement rocks.

north-vergent thin-skinned thrusts which sole at depths of about 4–6 km (Fig. 2), based on the regional seismicity of the region (Webb and Kanamori, 1985) and balanced geologic cross-sections (Medwedeff, 1988, 1992). Structures in the upper 7 km of crust have propagated northwards into the thick sequence of Neogene sediments in the southern San Joaquin Valley; they are expressed as the active Pleito Thrust which breaks the surface to the south (Hall, 1984), and blind faults which underlie active folds, including Wheeler Ridge to the north. A major thick-skinned structure, the White Wolf fault, also accommodates shortening in the region and is defined as a north-vergent, basement-involved, high-angle thrust and overlying fold (Fig. 2).

Wheeler Ridge has formed above a north-vergent wedge thrust (Fig. 3), whose subsurface geometry is tightly constrained where abundant oil well and seismic data are present at its eastern end (Fig. 4). The geometry of the faults which underlie Wheeler Ridge are best described as a north-vergent thrust wedge (Fig. 4; Medwedeff, 1992), with a south-dipping, structurally lower thrust and north-dipping upper thrust. The lower thrust has a simple, planar geometry; the upper thrust varies abruptly along strike to the east, across a series of N-trending tear faults, first recognized by Medwedeff (1992) and later studied in more detail by Mueller and Talling (1997). The tear faults documented both in the subsurface and on the surface correspond with the location of the wind and water gaps and illustrate the link between the three dimensional structural evolution of the fold and its late Quaternary syntectonic depositional and erosional history.

Although complex at an oilfield scale (Medwedeff, 1992), the simplified geometry of eastern Wheeler Ridge is that of a north-vergent, eastward plunging anticline with a steep, north-dipping front limb and a broader, more shallowly-inclined back limb. The crest of the fold varies from a sharp anticlinal hinge in the west to an increasingly broad and flat plunge panel to the east. Wind and water gaps which traverse the fold have valley floors that decrease in elevation from west to east (Shelton, 1966). The topography of Wheeler Ridge also coincides with a decrease in structural relief from west to east, which was documented in the subsurface by Medwedeff (1992) and interpreted to indicate eastward propagation of the fold. In addition, work by Zepeda *et al.* (1996) determined that geomorphic surfaces on the crest of Wheeler Ridge decrease in age from west to east, confirming that the fold is actively propagating to the east.

The kinematic implications of this observation are that Wheeler Ridge anticline is migrating both north and east as displacement builds on the underlying blind thrusts. From a geomorphic and depositional standpoint, the record of incremental folding events at Wheeler Ridge is recorded in syntectonic alluvial sediments deposited as small alluvial fans fed by drainages on the front limb of the fold and by much larger drainage basins which funnel sediment through water and wind gaps which cut the fold.

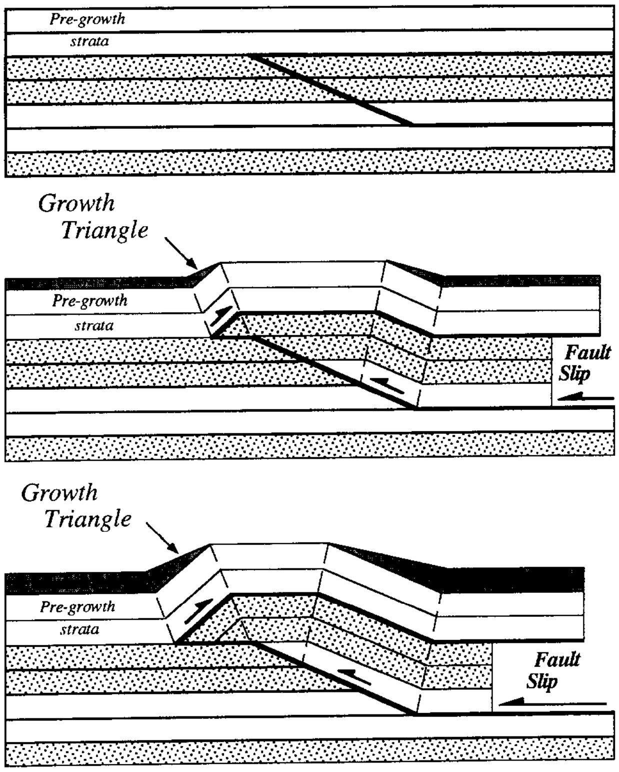

Fig. 3. Sequential series of simplified cross-sections illustrating the evolution of a wedge thrust structure. In this example, uplift exceeds burial and about half of the structural relief of the fold is apparent at the surface. Note the growth sediments which form triangular-shaped features termed 'growth triangles' (Suppe *et al.*, 1991) which are predicted to be preserved on the front and back limbs of the fold (Medwedeff, 1992). The most important information regarding short-term fold growth is contained on the geomorphic surface which bounds the top of the growth triangle on the front limb of Wheeler Ridge. This surface, termed the growth axial surface is the locus of points which once lay at the base of the front limb, where the fold limb above the wedge thrust is actively moving by kink-band migration, consuming undeformed material in front of the fold.

GROWTH STRATIGRAPHY

Syntectonic strata that interact with and record growth of Wheeler Ridge anticline are derived from coarse-grained conglomerate and gravel of the late Quaternary Tulare Formation, a unit deposited as large coalesced alluvial fans that flank the San Emigdio Mountains (Fig. 1). The present network of active drainages which extends downslope from the hinterland of the thrust belt is either deflected to the east around Wheeler Ridge, or into transverse drainages that cut across the fold (Burbank and Verges, 1994). Other syntectonic sediment is derived from more locally restricted drainages which are incised into the crest and limbs of the fold. Alluvial fans sourced from drainages on the front limb and crest of Wheeler Ridge are small in area and located at the abrupt change in slope that marks the northern edge of the fold, both topographically and in the subsurface (Medwedeff, 1992). Fans fed from transverse drainages that cross Wheeler Ridge cover broader areas of its front limb where they extend outward onto the alluvial plain to the north. The two largest alluvial fans preserved along the front limb of the fold occur at the mouths of prominent wind and water gaps.

Since the introduction of livestock into the region in the 1850s, the rate of sedimentation on alluvial fans has increased as a result of denudation of hillslope plants and grasses. Trenches excavated on the distal portions of the youngest fans mapped along the north-facing limb of Wheeler Ridge (Fig. 6) contain an overlying 1 m thick deposit of pebble conglomerate and gravel. This overlies fine-grained silts which we interpret to pre-date the onset of increased denudation in the area.

We have followed the alluvial chronology of Zepeda *et al.* (1996) who mapped alluvial deposits based on the degree of soil development in them, a technique used to define the age of deformed geomorphic surfaces (Birkeland, 1984). Their age constraints include ^{14}C analyses of charcoal, and Uranium Series dating of pedogenic carbonate from the crest of the fold, which they use to broadly define rates (*ca* $\pm 25\%$; Birkeland, 1984) of uplift and eastward propagation. They defined the age of older geomorphic surfaces in two ways; (1) by extrapolating the age of young well-dated deposits uplifted at the eastern end of the fold, using the dip of the plunge panel (or elevation of the fold crest) defined by Medwedeff (1992) as a guide; and (2) by comparing the soil profiles found on these older, more elevated surfaces with other, better dated soil chronosequences in the southern San Joaquin Valley (Harden, 1982).

GEOMORPHOLOGY OF THE FRONT LIMB

Terraced hillslopes

The front limb of Wheeler Ridge anticline contains a number of geomorphic landforms that may have been produced by active kink-band migration, the dominant process which acts to build the fold (Medwedeff, 1992; Figs 5–8). The most striking aspect of the front limb are flights of regularly-spaced terraces, which are typically 2–4 m in width and separated by 9–12 m wide risers, measured parallel to the ground surface (Fig. 8a–d).

Terrace flights are readily apparent on 1:25,000 scale aerial photographs, and occur on the north-facing front limbs of a number of active folds (Medwedeff *et al.*, 1993), along the leading edge of the Transverse Ranges fold and thrust belt (Fig. 1). These folds include Wheeler Ridge, the San Emigdio Mountains, the Los Lobos folds and other structures further west and north in the southwestern San Joaquin Valley (Fig. 1). Less well-developed terraces are also preserved along drainage channel walls incised into the interior of Kettleman Dome, an active fold located 150 km to the northwest in the west-central San Joaquin Valley.

At Wheeler Ridge, the terraces are subparallel to the front limb of the fold and have treads (the flat terrace surfaces) that are variably inclined (Fig. 8a–d). Terrace treads high on the fold limb (see area mapped in Fig. 6)

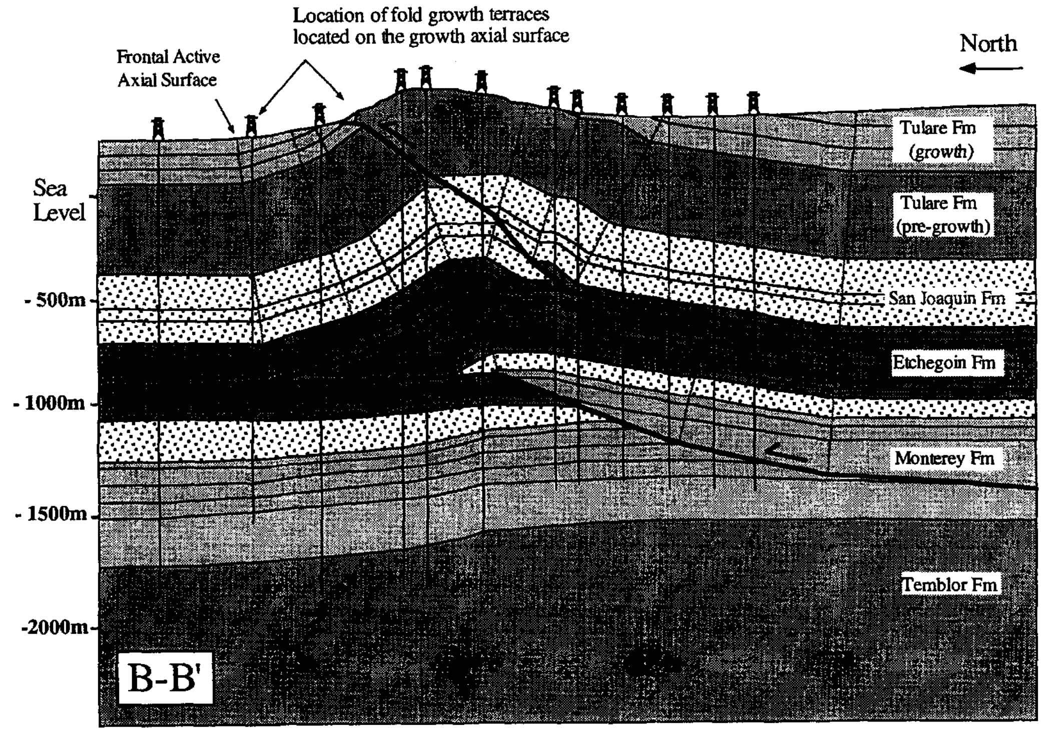

Fig. 4. Cross-section B–B′ through the eastern part of Wheeler Ridge anticline modified from Medwedeff (1992). Note the tightly constrained nature of the solution, which utilizes closely-spaced well data from a producing oilfield projected along the plunge of the fold. Location of section shown on Fig. 1.

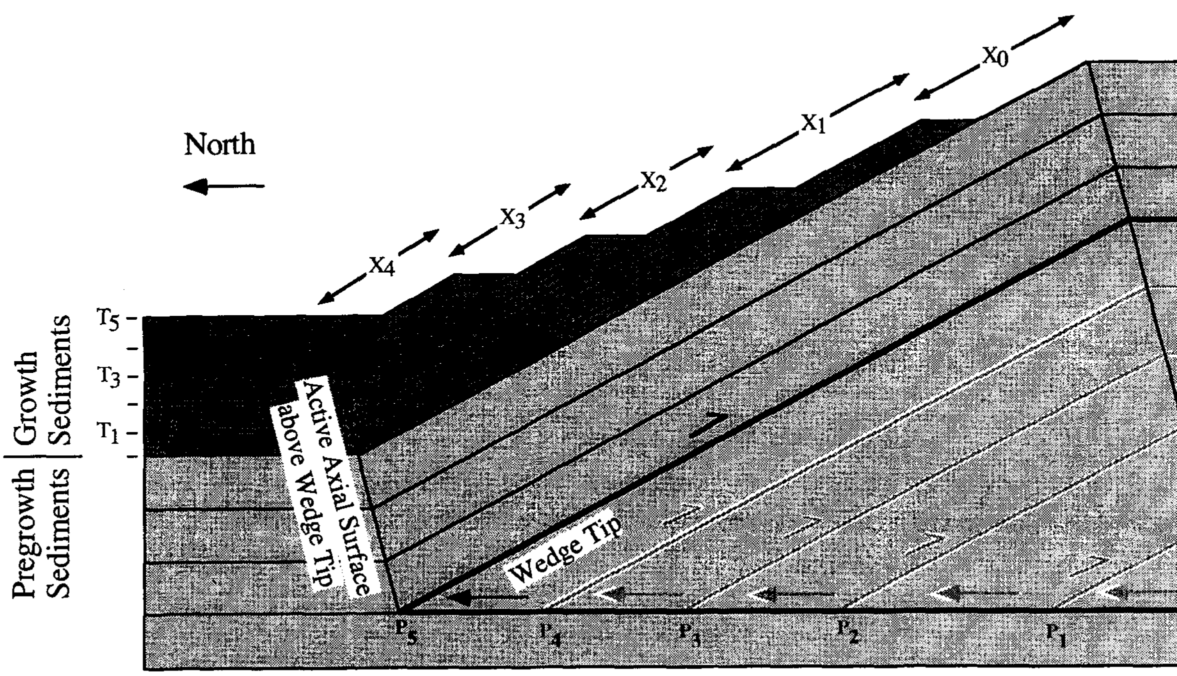

Fig. 5. Simplified model of a terraced hillslope formed on the front limb of a partly buried wedge thrust structure. Folding events occur at times T_n, defined by onlapped sediment packages. Terraces develop above sediments deposited above strata which have already been folded through an active axial surface. Limb widening per event is denoted by X_n, which is measured parallel to bedding between outer terrace edges.

are steeply inclined in a direction parallel to the axis of the fold. This part of the fold limb lies in the hangingwall of a south-dipping thrust mapped in the subsurface by Medwedeff (1992) that breaks the surface. Terrace treads preserved further downslope on the footwall of the emergent thrust are nearly flat along much of their lengths (Fig. 6). Terraces in the hangingwall of the emergent thrust are truncated by the trace of the fault.

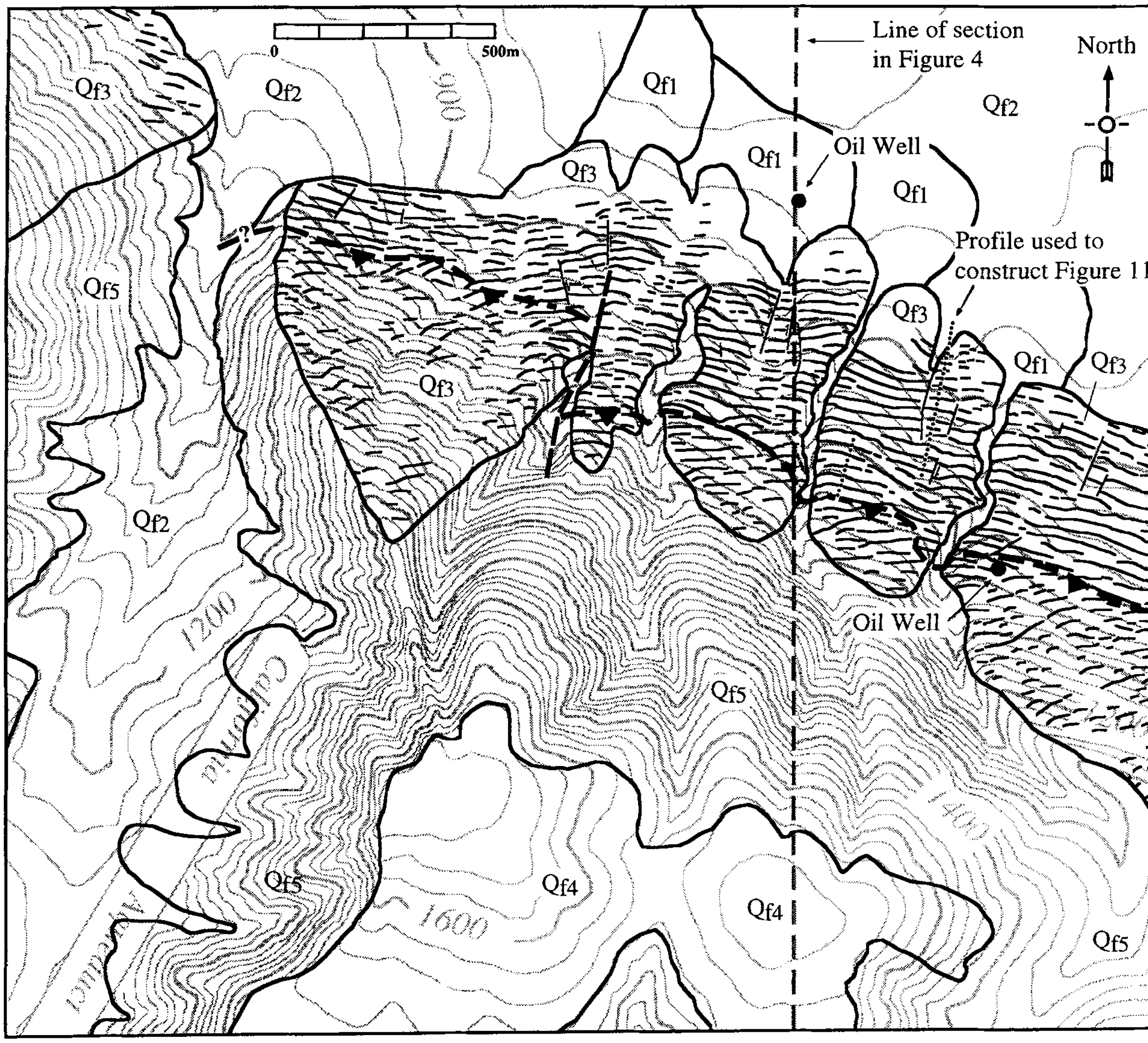

Fig. 6. Map of Late Quaternary alluvial and folding-related landforms on the front limb of eastern Wheeler Ridge anticline.

The terraces do not appear to cross one another (Fig. 6). Gullies incised into the front limb of Wheeler Ridge typically truncate terraces, although some terraces appear to wrap around the upper portions of gully walls, forming blunt, south-pointing 'v's. A few terraces terminate abruptly along strike on the front limb between adjacent risers that merge beyond the intervening terrace termination (Fig. 8b). Other terraces appear to be laterally offset across small displacement faults that strike north–south across the front limb (Fig. 6).

Terraces are only preserved along the base of the north-facing side of Wheeler Ridge, where work by Medwedeff (1992) predicts active migration of the front limb (Fig. 6). They are not present in alluvial deposits of similar age on the south limb of the fold, or on the walls of major canyons which cut the fold. They are also not observed on gently inclined alluvial fans which exit the mouths of canyons forming wind and water gaps, or the very young (post-1860?) fans which are actively forming at the base of the front limb.

Terrace flights preserved along Wheeler Ridge and the San Emigdio Mountains have varying morphology related to their position on the front limb. Terraces at the base of these fold limbs generally have sharp outer edges which become increasing more diffuse and eroded at higher positions on the structure (Fig. 8c). The width of a terrace flight coincides with the dip of the fold limb where they are preserved; steeper portions of the front limb typically preserve fewer numbers of terraces than on more gently dipping ones.

Stratigraphic information for the origin of the terraces is obscured by extensive bioturbation by a species of ground squirrel that completely reworks the upper 1–3 m of strata in deposits older than 1 Ka (Zepeda *et al.*, 1996). In a trench excavated for the purpose of examining young sediments immediately beneath the terraces (see location on Fig. 6), the upper 2–3 m of gravelly parent material was extensively bioturbated. However, undisturbed strata at depths of greater than 3 m were inclined parallel to overlying terrace risers. Soil stratigraphy in the trench

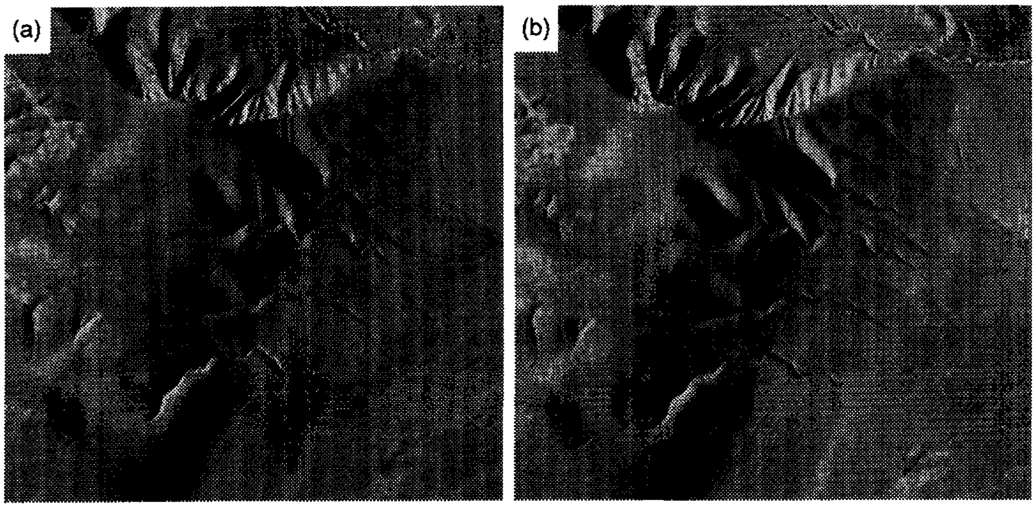

Fig. 7. Stereopair of area mapped in Fig. 6. Note the corrugated surface in the center-right of the photos that contains alluvial ridges with incised drainages located on their crests. These lie on the steeply dipping front limb of Wheeler Ridge.

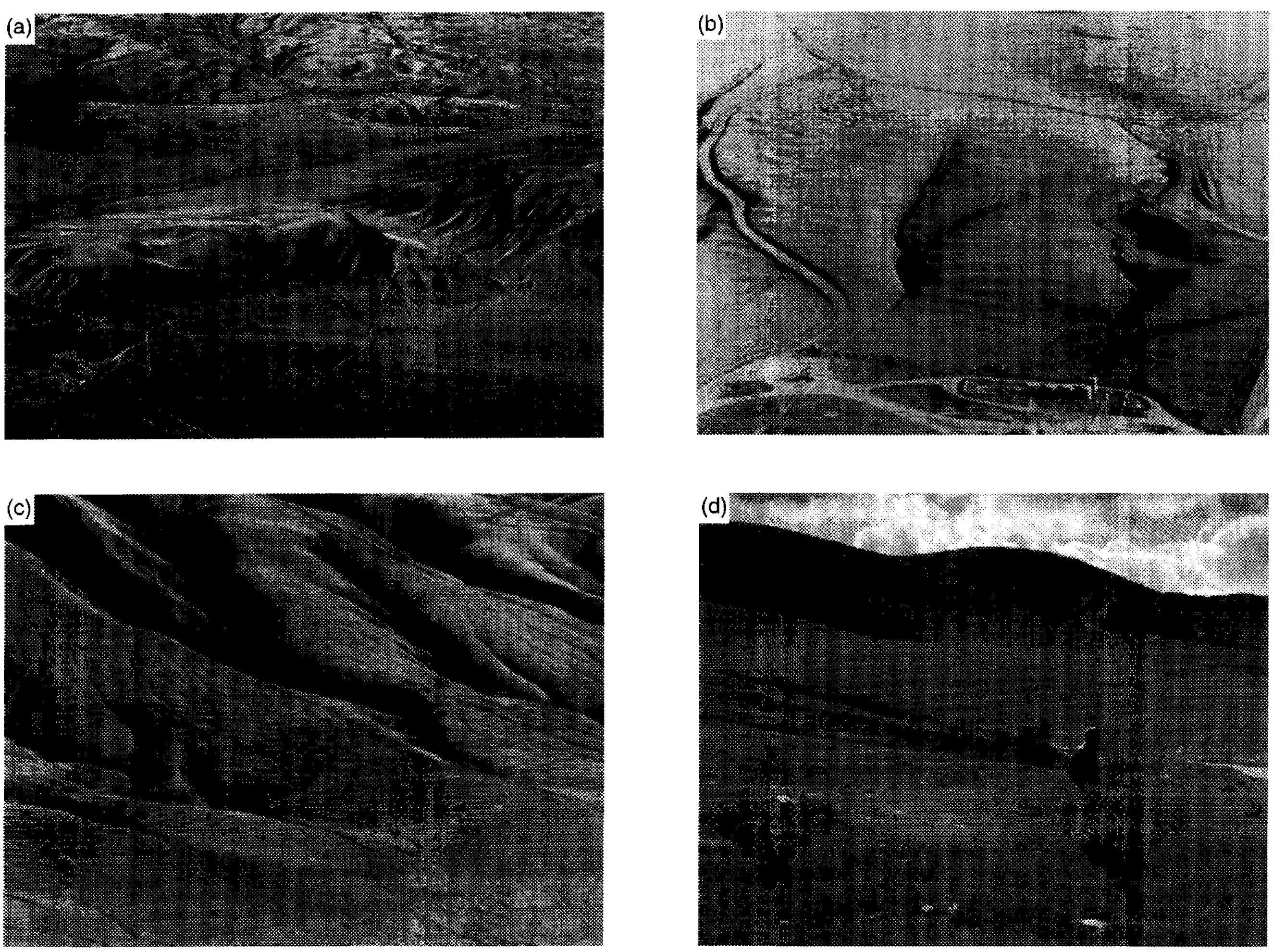

Fig. 8. Oblique aerial and ground photos of eastern Wheeler Ridge (clockwise from upper left). (a) is viewed south at the front limb of Wheeler Ridge prior to excavation of a gravel quarry (1957 photo courtesy of John Shelton, negative No. 697). Note the terraces which appear as narrow light lines on the front limb of the fold. (b) is viewed at a low altitude to the southwest at the easternmost part of Wheeler Ridge. The front limb of the fold is the surface dipping towards the viewer that is covered with light-colored terraces and darker terrace risers. Note the increasingly diffused character of the terraces at higher positions on the fold limb, which is also apparent in (c), which is located further east. (d) is viewed southwest at the site of the trench excavation, which lies immediately behind the elongate spoil pile. Note the scale of the backhoe in comparison to the terraces, and terrace risers.

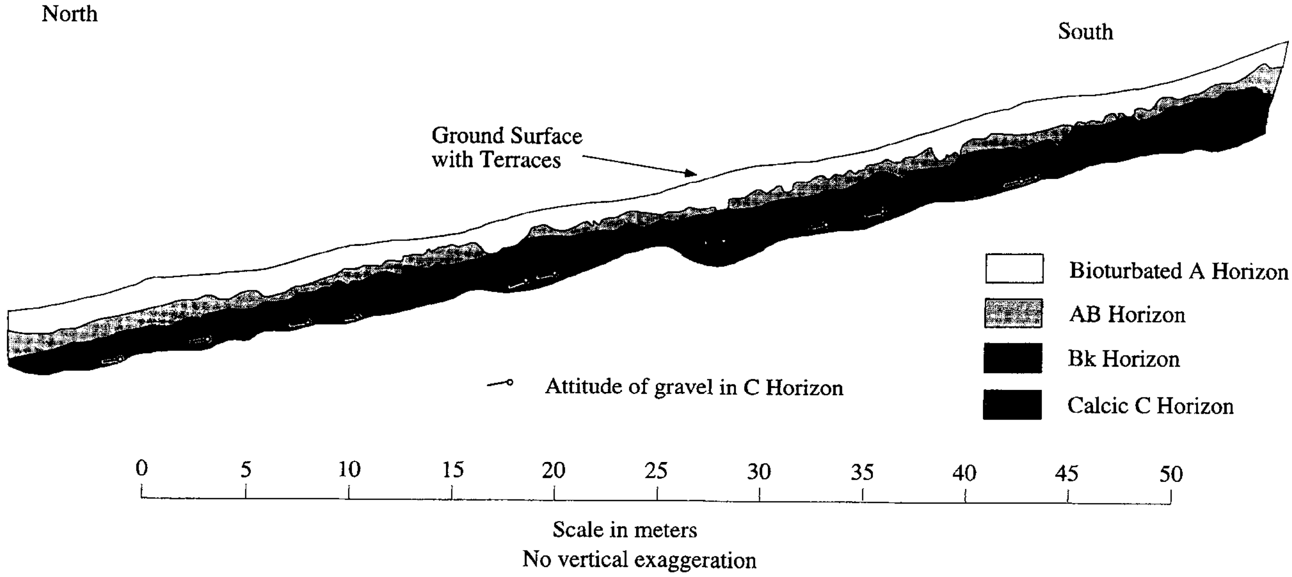

Fig. 9. Log of east wall of 5 m deep trench excavated at the base of the front limb of Wheeler Ridge, east of the prominent transverse drainage located in the right-center of Fig. 8(a). Location of trench is marked on Figs 1 and 8(d). Note the morphology of the terraces, apparent in cross-section as the upper ground surface. Primary alluvial sediments are not preserved in the upper 23 m of the trench due to bioturbation. However, attitudes of alluvial fan sediments, at greater depths are parallel to overlying terrace risers as predicted in the model shown in Fig. 5. Note also the buried Argillic Bk horizon preserved in the upper part of the trench that we interpret to record an older alluvial fan surface that has been subsequently bent into the fold limb.

included a buried argillic horizon that terminated downslope as a thinly tapered wedge (Fig. 9).

Alluvial ridges

Other landforms formed on the front limb of Wheeler Ridge include elongate ridges of alluvial sediment oriented N9°E which form distinctive corrugations that are apparent on 1:24,000 scale topographic maps and aerial photographs (Figs 6 & 7). The crests of these features are elevated 6–8 m above adjacent areas on the fold limb. In the area mapped on Fig. 6, they are about 150–200 m wide and extend 250–300 m up the front limb of the fold (see also Fig. 7). A remarkably distinctive aspect of the alluvial ridges include incised drainages which extend along their crests, that drain small catchment areas incised into the crest and front limb of the anticline (Fig. 7).

Small alluvial fans are formed at points where incised drainages on the crest of the ridges exit onto the undeformed plain north of the front limb of Wheeler Ridge (Q1 on Fig. 6). The width of these young fans is similar or slightly greater than the alluvial ridges they lie downslope from. Sediments exposed in natural gully exposures incised into the alluvial ridges, and in a trench excavated on the fold limb are comprised of parallel-bedded gravels and conglomerate. These strata are similar to modern fan deposits exposed in a gravel quarry in the eastern part of Wheeler Ridge and along channel walls incised into large modern fans located at the mouths of wind and water gaps.

GEOMORPHIC MODELS

Alluvial ridges

We interpret the alluvial sediment ridges on the front limb of Wheeler Ridge to form as gently-dipping alluvial fans deposited at the base of the fold limb which are subsequently bent upward as the thrust wedge tip migrates to the north (Fig. 10). Channel incision of the more steeply inclined fan surfaces then occurs, and new fans are formed basinward. As the fold limb migrates in a lengthening kink-band, continued sedimentation produces the incised ridges composed of alluvial fan sediments. An observation which supports this model includes the parallel-bedded nature of deposits comprising the alluvial ridges which are clearly deposited in an alluvial fan environment. The width of the modern fans formed at the base of the front limb is similar to the ridges, also supporting the hypothesis. Other evidence for the model is provided by a buried argillic (Bk) horizon, documented in a trench excavated at the base of the front limb (Fig. 9) that we interpret to support the concept of shingled alluvial fan surfaces that are progressively bent upward and incorporated into the fold.

An implication of our model is that the axis of a single shingled sequence of fans can be used as a finite strain marker, effectively recording the sense of limb widening which we equate to the direction of slip on the underlying blind thrust (Fig. 7). Mapping of the axes of four alluvial ridges located on Fig. 6 indicates a consistent direction of oblique fold growth, apparent where the apex of shingled fan sequences have a rake of 84° (towards the west) relative to the strike of the fold. This indicates the

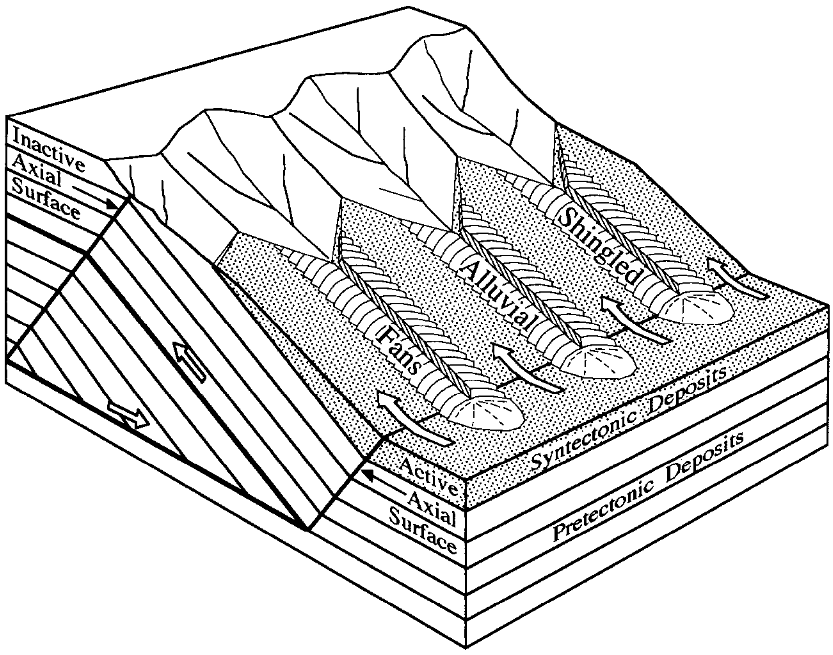

Fig. 10. Block diagram illustrating the architecture of alluvial sediments on the front limb of Wheeler Ridge. Note the shallow wedge thrust at depth that migrates to the north, continually incorporating alluval fan deposits into the front limb. The unique aspect of the alluvial ridges are the incised drainages located along their crests. See Fig. 7 for stereopairs of these features.

component of left lateral slip for the underlying blind thrust, which is about 11% of the dip-slip component.

This is not surprising for E–W-oriented thrusts in the Transverse Ranges, where both earthquake focal mechanisms (Gutenberg, 1955), and outcrop scale strain in fault-related folds (Geotechnical Consultants Inc., 1977), indicates a minor sinistral component of fault slip. The most apparent examples of this process include: (1) the focal mechanism for the 1952 M7.6 White Wolf Earthquake, which originated on the White Wolf fault beneath Wheeler Ridge; (2) numerous small-displacement strike-slip faults in trenches exposed in a small fold on the south limb of the Ventura Avenue Anticline; and (3) faults exposed in trenches located along the south limb of the Santa Monica anticlinorium, which bounds the northern edge of the Los Angeles Basin (J. Dolan, personal communication, 1994).

Terraced hillslopes

The front limb of Wheeler Ridge anticline has been documented to form by kink-band migration above a northward-migrating thrust wedge (Medwedeff, 1992), which lies 2 km beneath the surface. In addition, syntectonic sediment has been deposited along the base of the front limb by small drainages incised into the fold and by transverse drainages which carry sediment from the hinterland of the thrust belt. These 'growth' sediments thus interact with the narrow zone of folding, or active axial surface (Suppe *et al.*, 1991), located at the base of the fold which separates the north-dipping front limb of Wheeler Ridge from undeformed material lying in the alluvial plain to the north. The kinematic implication of this geometry is that material deposited along the base of the front limb is swept upward during migration of the active axial surface.

We envisage folding to occur as coseismic 'events' caused by sudden uplift during episodic earthquakes on the blind thrust that underlies the fold, similar to historic thrust-type earthquakes which were accompanied by folding (Yielding *et al.*, 1981; Philip *et al.*, 1992; Treiman, 1995). Although several deformational processes accommodate earthquake-related growth of fault-bend folds (see discussion in the Introduction), we suggest the formation of kink-bands along active axial surfaces may be a dominant mechanism at Wheeler Ridge because significant bed thickening in its front limb has not been recorded (Medwedeff, 1992). The front limb of Wheeler Ridge is thus predicted to grow by the formation of an elongate kink-band along its base, similar to the surface deformation that occurred above a blind thrust during the 1995 Northridge earthquake (Treiman, 1995).

For a wedge thrust that undergoes syntectonic burial along the base of its front limb, we predict that upward propagation of the active axial surface through onlapped alluvial sediment deposited during an interseismic period will create a prism of uplifted, but otherwise undeformed strata (Fig. 5). Our model suggests this will produce a terrace-like feature whose outer edge marks the former position of the active axial surface, prior to the folding event (Fig. 5). The terrace forms the upper surface of syntectonic sediment onlapped above material already bent into the front limb. The model also predicts that the distance between the outer edges of adjacent terraces, measured parallel to bedding, is equivalent to the amount of fault slip released during the earthquake on the underlying blind thrust (Fig. 4).

Support for a folding-related origin of the terraces on the front limb of Wheeler Ridge is based on their morphology, location on the fold and the kinematics implied by subsurface studies (Medwedeff, 1992). The terraces are clearly more eroded and diffuse with higher positions on the front limb, implying their progressively greater age as they have migrated upward (Fig. 8c). We interpret this as important evidence that these features have formed at the base of the fold and been subsequently carried upward during northward migration of its front limb. The terraces are also located only on the front limb of Wheeler Ridge, where active kink-band migration is predicted to occur, based on tightly constrained subsurface data. In addition, strata exposed in a trench excavated across the terraces have similar orientations to adjacent terrace risers, in accordance with the geometry predicted in the model (Figs 5 & 9). Also, sharp bending across a narrow active axial surface along the front limb of Wheeler Ridge is likely to be facilitated by the short 1100 m distance between the ground and the wedge tip at depth (Fig. 4).

Alternative hypotheses for terraced hillslopes

Bioturbative processes have destroyed alluvial bedding to depths of ~2.5 m (Zepeda *et al.*, 1996; Fig. 9) where our model predicts folding beneath the outer edge of the terraces (Fig. 5). Because this does not allow us to test this critical geometric aspect of the model, we propose other plausible origins for the terraces. These range from flexural slip faulting, lake shorelines, features caused by soil creep and erosive trails made by livestock.

Wheeler Ridge has been extensively grazed for the past 150 years, therefore the terraces on its front limb may be erosive trails caused by livestock (Howard and Higgins, 1987). However, the terraces are typically 2–4 m wide, an order of magnitude greater than livestock trails presently in the area now. The terraces also end abruptly, do not anastomoze, and are not present on other similarly inclined slopes around Wheeler Ridge, relations not apparent for modern livestock trails in the area today.

The terraces may also have been formed as lake shorelines, that were subsequently deformed by uplift of Wheeler Ridge (i.e. they are not presently horizontal). Arguments for a shoreline-related origin includes the extent of the terraces over the 45 km long belt of active folds, and their linear geometry (Figs 1 & 8). The chief argument against this hypothesis is the lack of other shoreline features at similar elevations around the remainder of southern San Joaquin Valley for a lake that would have had to occupy much of the southern San Joaquin Valley (about half of the size of the Great Salt Lake), based on the regional topography of the basin.

Other terrace-like landforms have been documented to form by solifluction, where soil creeps downhill in saturated masses (Vincent and Clarke, 1976; Selby, 1993). This is an attractive alternative hypothesis for the terraces, because of the 2 m thick A horizons documented there that might be de-laminated from the underlying argillic horizons. However, the geometry of solifluction masses documented elsewhere (Washburn, 1947; Selby, 1993) argue against this, they typically are lobate in map view and have over-steepened fronts, unlike the features at Wheeler Ridge (Fig. 9). They also are not common outside of high-latitude periglacial areas, where delamination on slopes occurs above a permafrost layer.

The last alternative hypothesis we have considered for the origin of the fold growth terraces is tectonic, and related to flexural slip faulting caused by migration of material through the active axial surface now buried at the base of the front limb. Flexural slip faulting has been documented in active fault-related folds and appears to be an important deformation mechanism which accommodates fold growth (Klinger and Rockwell, 1989; Treiman, 1995). In this model, the terraces could be interpreted as front limbs on many evenly-spaced, top-to-the-south thrusts which deform the growth axial surface on the front limb of Wheeler Ridge. Evidence against a flexural slip faulting origin for the terraces are: (1) no faults were observed in the trench excavation which cut through bedding; (2) examples of flexural slip faults caused by folding during earthquakes such as the recent Northridge event (Treiman, 1995) are not as evenly spaced as the terraces at Wheeler Ridge; and (3) the subsurface geometry defined by well data suggests a concave-up geometry for the front limb which is unlikely to produce flexural slip faulting across bedding near the ground surface.

DISCUSSION

Earthquake behaviour on blind thrusts

If our proposed folding-related origin for the terraces is correct, Wheeler Ridge and other active folds along the leading edge of the thrust belt preserve remarkably long records of past earthquakes. Based on our initial mapping and examination of the terraces, they are preserved in sediments as old as 65 Ka (Zepeda *et al.*, 1996).

Using the best age constraints available (Zepeda *et al.*, 1996), we calculate the terraces at the eastern end of Wheeler Ridge have a maximum recurrence interval of *ca* 500 years. This is based on the 14 Ka age constraint for the plunge panel at the eastern end of the fold (Zepeda *et al.*, 1996), a fault geometry at depth consistent with Medwedeff's cross-section number 6 (Medwedeff, 1992) and burial of the base of the front limb by a large alluvial fan fed by a transverse drainage. We also use these same data to determine a fault slip rate on the order of *ca* 10 mm year^{-1}, a rapid rate for individual thrusts in the Transverse Ranges.

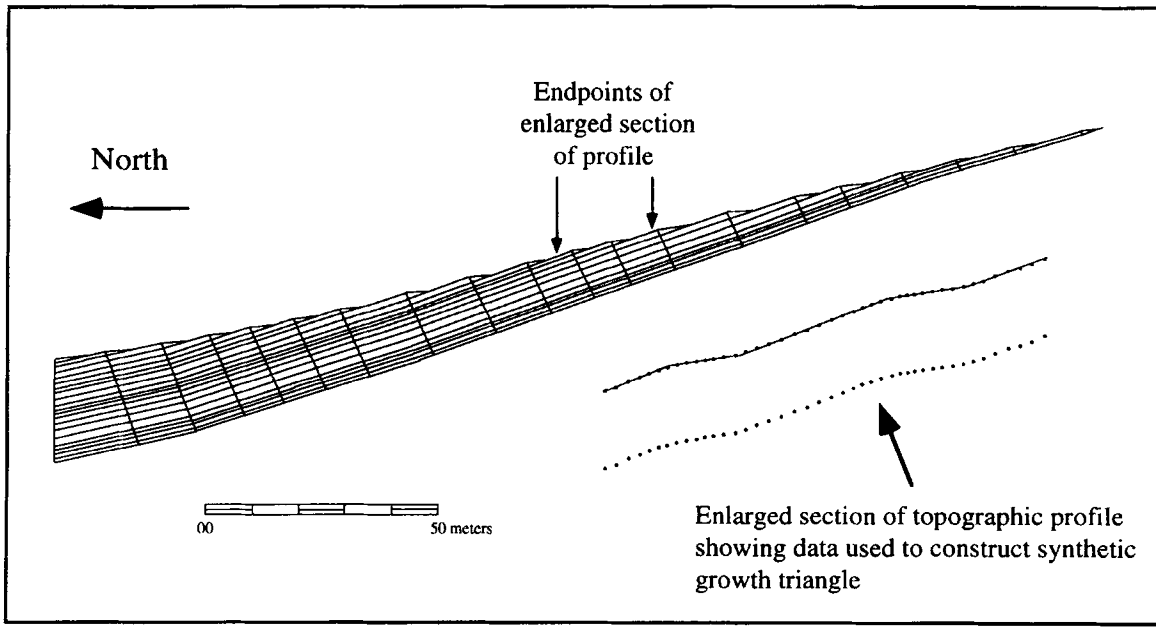

Fig. 11. Simplified cross-section of growth sediments and fold growth terraces derived from topographic profiles measured with a Wild Total Station (see location on Fig. 6). The 'synthetic growth triangle' defines the former positions of the active axial surface by the outer edge of each terrace. The distance between adjacent axial surfaces measured parallel to bedding provides values of X_n used to construct Fig. 12. The topographic profile is here simplified as straight line segments; the spacing of actual elevation points is shown in the enlarged insert.

Magnitude of events

The single most remarkable aspect of the fold growth terraces preserved at Wheeler Ridge, assuming their proposed origin during thrust-related earthquakes, is the magnitude of fault slip implied by their geometry. Construction of a synthetic growth triangle (Fig. 11), which is supported by subsurface well data and near-surface trenching data, yields 'folding events' caused by an average of 10 m of displacement on the underlying blind thrust (Fig. 12).

For the available empirical dataset in southern California (Dolan *et al.*, 1995), which relates surface slip with the magnitude of individual earthquakes, 10 m of fault slip corresponds to an event greater than M8.0 (Fig. 13). Global comparisons of fault area vs earthquake magnitude (Wells and Coppersmith, 1994) indicate that M8.0 earthquakes are associated with faults having surface areas of 10,000 km^2. Using a 1000 km^2 value for the area (fault length × fault width) of the basal décollement in the region (Fig. 2) and the depth of seismogenic crust, we calculate that the thrust belt is, at most, capable of a M7.0 seismic event using the regressions of Wells and Coppersmith (1994).

This is clearly much less than the magnitude of folding events implied by the fold growth terraces. We attribute this difference to three possibilities, either: (1) the terraces are formed by processes other than that outlined in our folding model; (2) events are regularly clustered in time, beyond our ability to distinguish events with the available growth stratigraphy (i.e. each terrace corresponds to only a fraction of the earthquakes which have built Wheeler Ridge); or (3) the faults along the leading edge of the thrust belt are part of a much larger system of linked structures.

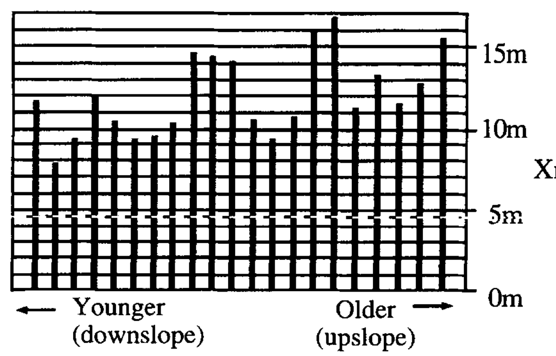

Fig. 12. Histogram of the magnitude of limb-widening events (X_n) measured from the synthetic growth triangle shown on Fig. 11. We interpret the regular terrace spacing to record periodic earthquakes on the blind thrust which underlies the fold. The large ~10 m distance between terraces indicates either: (1) ~M8.0 earthquakes at regular intervals on the underlying blind thrust, (2) clustered ~M7.5 earthquakes on the blind thrust, or (3) the terraces are formed by processes other than that illustrated in Fig. 5. Terrace risers of even greater width (e.g ~14 m) are located where terraces terminate laterally; thus they are probably composite in character and may not correspond to individual events.

Because the leading edge of the Transverse Ranges is being deformed in response to shortening across the onset of the 'Big Bend', the major restraining bend in the San Andreas fault system, we suggest the thrust belt may be recording events of much greater magnitude than expected if considered as an isolated fault system. A

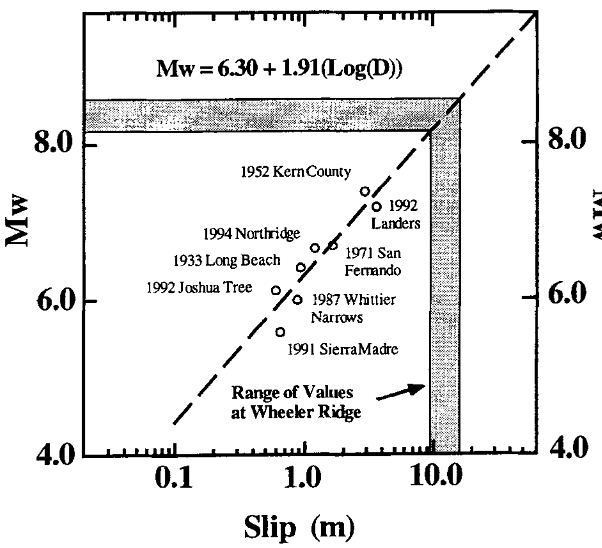

Fig. 13. Regression from Dolan *et al.* (1995) which defines the relationship between magnitude and surface displacement for recent historic earthquakes in southern California. The range of values for limb widening events defined by surveyed topographic profiles at Wheeler Ridge is about 10–14 m per event, which we equate to fault slip at depth based on fault-related fold theory (Suppe, 1983) and the assumption that each terrace is formed by only one event. An alternative hypothesis is that the terraces are separated by several small, clustered events (e.g. M7.5, rather than M8.0). The apparent disparity between magnitude and rupture length (the blind thrusts which produce the fold growth terraces are <45 km long) may indicate that the thrust earthquakes are kinematically linked with much larger events which originate on the nearby San Andreas fault which drives crustal shortening in this region.

historic analog for this idea is illustrated by the pattern of surface rupture caused by the 1957 M8.3 Gobi–Altai earthquake in Mongolia (Baljinnyam *et al.*, 1993; Bayarsayhan *et al.*, 1996, Fig. 14). During that earthquake, thrust faults with up to 9.2 m of dip-slip broke the surface at restraining bends along the main fault. The main strand of the strike-slip fault itself displayed a maximum of 8 m of slip. The apparent increase in slip on the thrusts during the Gobi Altai event may be related to the geometry of the linked lateral and thrust system; we expect pure strike-slip to translate to similar amounts of heave and commensurately greater amounts of total slip on dipping thrust faults, depending on their inclinations.

Studies of the San Andreas in the nearby Carrizo Plain (Grant, 1993; Grant and Sieh, 1993, 1994) indicate that the most recent events on the fault were associated with about 9 m of strike-slip. Therefore, it is possible that the size of folding 'events' we interpret to be recorded at Wheeler Ridge are within the realm of slip magnitude documented on the nearby Carrizo segment of the San Andreas fault.

CONCLUSIONS

In conclusion, our studies show that fault-related folds may grow by geologically instantaneous folding 'events' related to earthquakes on underlying blind thrusts. Also, by coupling classic studies of fold geometry (Medwedeff, 1992), with work on growth sediments shed off rising folds which are deformed into unique landforms, insight is gained on mechanisms of fold growth. For Wheeler Ridge, growth of the fold is clearly dominated by kink-band migration. In addition, alluvial ridges on the front limb of the fold illustrate a component of lateral slip on the underlying blind thrust not readily identified by other methods.

Unambiguous identification of unique landforms formed by active kink-band migration, such as alluvial ridges, or terraced fold limbs increases confidence in

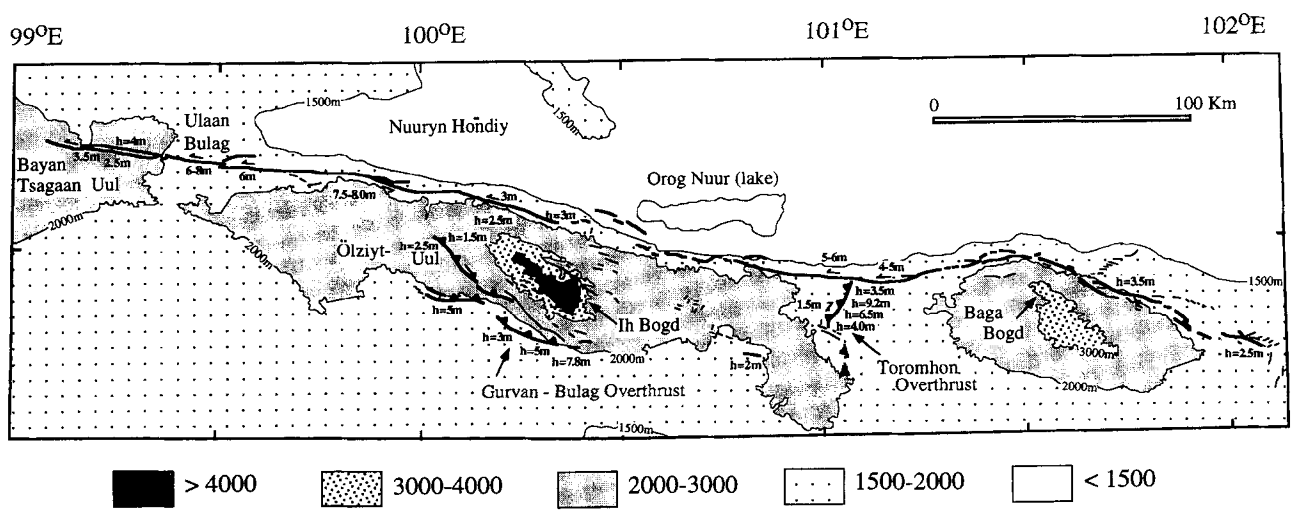

Fig. 14. Map of surface ruptures associated with the 1957 M8.3 Gobi Altai earthquake in Mongolia modified from Baljinnyam *et al.* (1993). Note the amount of surface displacement on the Gurvan Bulag and Toromhon thrusts (up to 9.2 m) which exceeds the maximum 8 m displacement measured along the main strike-slip rupture. We consider this as a possible analog for thrusts and folds such as Wheeler Ridge which are driven by shortening across the big bend in the San Andreas fault.

assigning particular deformation mechanisms used to balance geologic cross-sections, particularly in areas of little subsurface control. Most 2-D balancing methods also assume plane strain, the validity of which can be tested with the geomorphic features we have described.

The regional implications of our work suggests that strain in thrust belts may be dynamically linked, or coupled during earthquakes, especially where it is driven by shortening along restraining bends across great strike-slip faults such as the San Andreas. In addition, the component of horizontal shortening across these thrust belts may actually be slightly greater than lateral slip apparent at the surface on the driving strike-slip fault system.

Acknowledgements—We thank Woody Pollard, Maria Hertzberg, Frank Bilotti and Enrique Novoa for help with trenching operations, surveying and soil descriptions. Access to Wheeler Ridge was provided by Jeff Stephenson of the Dale Poe Development Corporation, whose help we gratefully acknowledge. The manuscript was improved from reviews by Ramon Arrowsmith, John Spang and Eric Erslev. We also thank the Southern California Earthquake Center for providing funding for other research on active folding that contributed to our understanding of folding-related landforms at Wheeler Ridge.

REFERENCES

Baljinnyam, I., Bayasgalan, A., Bodsov, B. A., Cisternas, A., Dem'yanovich, Ganbaatar, L., Kocketkov, V. M., Kurushin, R. A., Molnar, P., Philip, H. and Vashchilov, Y. (1993) Ruptures of major earthquakes and active deformation in Mongolia and its surroundings. *Geological Society, America Memoir* **181**, 1–62.

Bayarsayhan, C., Bayagalan, A., Enhtuvshin, B., Hudnut, K., Kurushin, R. A., Molnar, P. and Olziybat, M. (1996) 1957 Gobi–Altay, Mongolia, earthquake as a prototype for southern California's most devastating earthquake. *Geology* **24**, 579–582.

Birkeland, P. W. (1984) *Soils and Geomorphology*. Oxford University Press, New York.

Burbank, D.W. and Verges, J. (1994) Reconstruction of topography and related depositional systems during active thrusting. *Journal of Geophysical Research* **99**, 20,281–20,297.

Dolan, J. F., Sieh, K., Rockwell, T. R., Yeats, R. S., Shaw, J., Suppe, J., Huftile, G. J. and Gath, E. M. (1995) Prospects of larger or more frequent earthquakes in the Los Angeles Metropolitan Region, California. *Science* **267**, 195-205.

Geotechnical Consultants, Inc. (1977) Geotechnical–Seismic Investigation of the Proposed 330 Zone Water Storage Reservoir and Water Conditioning Facilities for the City of San Buenaventura, California. Consultants Report V77151.

Grant, L. B. (1993) Characterization of large earthquakes on the San Andreas Fault in the Carrizo Plain; implications for fault mechanics ands seismic hazard. PhD thesis, California Institute of Technology.

Grant, L. B. and Sieh, K. (1993) Stratigraphic evidence for seven meters of dextral slip on the San Andreas Fault during the 1857 earthquake in the Carrizo Plain. *Bulletin of the Seismology Society, America* **83**, 619–635.

Grant, L. B. and Sieh, K. (1994) Paleoseismic evidence of clustered earthquakes on the San Andreas fault in the Carrizo Plain, California. *Journal of Geophysical Research* **99**, 6819–6841.

Gutenberg, B. (1955) The first motion on longitudinal and transverse waves of the main shock and the direction of slip. *California Division of Mines and Geology Bulletin* **171**, 165–170.

Hall, N. T. (1984) Late Quaternary history of the eastern Pleito thrust fault, northern Transverse Ranges, California. Ph.D. thesis, Stanford University.

Harden, J. W. (1982) A quantitative index of soil development from field descriptions: Examples from a chronosequence in central California. *Geoderma* **28**, 1–28.

Hardy, S. and Poblett, J. (1994) Geometric and numerical models of progressive limb rotation in detachment folds. *Geology* **22**, 371–374.

Howard, J. K. and Higgins, C. G. (1987) Dimensions of grazing-step terracettes and their significance. In *International Geomorphology 1986, Proceedings of the 1st Conference*, ed. V. Gardinier, pp. 545–568. Wiley, Chichester.

Kelson, K. I., Simpson, G. D., VanArsdale, R. B., Haraden, C. C. and Lettis, W. R. (1996) Multiple late Holocene Earthquakes along the Reelfoot fault, central New Madrid seismic zone. *Journal of Geophysical Research* **101**, 6151–6170.

Klinger, R. E. and Rockwell, T. K. (1989) Flexural-slip folding along the Eastern Elmore Ranch Fault in the Superstition Hills Earthquake sequence of November 1987. *Bulletin of the Seismology Society, America* **79**, 297–303.

Laduzinsky, D. (1989) Late Pleistocene–Holocene chronology and tectonics, San Emigdio Mountains. M.Sc. thesis, University of California, Santa Barbara.

Medwedeff, D. A. (1988) Structural analysis and tectonic significance of late-Tertiary and Quaternary, compressive-growth folding, San Joaquin Valley, California. Ph.D. thesis, Princeton University, New Jersey.

Medwedeff, D. A. (1989) Growth fault-bend folding at the Southeast Lost Hills, San Joaquin Vcalley, California. *Bulletin of the American Association of Petroleum Geologists* **73**, 54–67.

Medwedeff, D. A. (1992), Geometry and kinematics of an active, laterally propagating wedge thrust, Wheeler Ridge, California. In *Structural Geology of Fold and Thrust Belts*, eds S. Mitra and G. Fisher, pp. 3–28. John Hopkins University Press, Baltimore.

Medwedeff, D. A., Lin, J. T. C., Carr, T. R. and Stafford, J. M. (1993) Superposition of basement involved structures and a detached thrust system: a model for existing and potential production in the San Emigdio Mountains, San Joaquin Valley, California. *Bulletin of the American Association of Petroleum Geologists (abstract)* **77**, 333.

Mueller K. J. and Talling, P. J. (1997) Geomorphic evidence for tear faults accommodating lateral propagation of an active fault-bend fold, Wheeler Ridge, California. *Journal of Structural Geology*, **19**, 397–411.

Namson, J. and Davis, T. L. (1988) Seismically active fold and thrust belt in the San Joaquin Valley, central California. *Bulletin of the Geoloical Society, America* **100**, 257–273.

Philip, H., Rogozhin, E., Cisternas, A., Bousquet, J. C., Borisov, B. and Karakhanian, A. (1992) The Armenian Earthquake of 1988 December 7: faulting and folding, neotectonics and palaeoseismicity. *Geophysics Journal International* **110**, 141–158.

Rich, J. L. (1934) Mechanics of low-angle Overthrust Faulting as illustrated by the Cumberland Thrust Block, Virginia, Kentucky, and Tennessee. *Bulletin of the American Association of Petroleum Geologists* **18**, 1584–1595.

Rockwell, T. K., Keller, E. A. and Dembroff, G. R. (1988) Quaternary rate of folding of the Ventura anticline, western Transverse Ranges, southern California. *Bulletin of the Geological Society, America* **100**, 850–858.

Seaver, D. B. (1986) Quaternary evolution and deformation of the San Emigdio Mountains and their alluvial fans, Transverse Ranges, California. M.A. thesis, Santa Barbara, University of California.

Selby, M. J. (1993) *Hillslope Materials and Processes*. Oxford University Press, Oxford.

Shaw, J. H., Bischke, R. E. and Suppe, J. (1992) Evaluation of the use of compressive growth structure in earthquake hazard assessment. U.S. Geological Survey Open-File Report 92-258.

Shaw, J. H. and Suppe, J. (1995) Earthquake hazards of active blind-thrust faults under the central Los Angeles basin, California. *Journal of Geophysical Research* **101**, 8623–8642.

Shelton, J. S. (1966) *Geology Illustrated*. Freeman, San Francisco.

Stein, R. S. and King, G. C. P. (1984) Seismic potential revealed by surface folding: 1983 Coalinga, California, earthquake. *Science* **224**, 869–872.

Stein, R. S. and Yeats, R. S. (1989) Hidden earthquakes. *Science America* **260**, 48–57.

Suppe, J. (1983) Geometry and kinematics of fault-bend folding. *American Journal of Science* **283**, 684–721.

Suppe, J., Chou, G. T. and Hook, S. C. (1991) Rates of folding and faulting determined from growth strata. In *Thrust Tectonics*, ed. K. R. McClay, pp. 105–121. Chapman and Hall, London.

Treiman, J. E. (1995) Surface Faulting near Santa Clarita. *Californian Division of Mines and Geology, Special Publication* **116**, 103–110.

Vincent, P. J. and Clarke, J. V. (1976) The terracette enigma: A review. *Biuletyn Peryglacjalny* **25**, 65–77.

Washburn, A. L. (1947) Reconnaissance geology of portions of Victoria Island and adjacent regions, Arctic Canada. *Geological Society of America Memoirs* **22**.

Webb, T. H. and Kanamori, H. (1985) Earthquake focal mechanisms in the eastern Transverse Ranges and San Emigdio Mountains, southern California and evidence for a regional décollement. *Bulletin of the Seismology Society, America* **75**, 737–758.

Wells, D. L. and Coppersmith, K. J. (1994) Updated empirical relationships between magnitude, rupture length, rupture area and surface displacement. *Bulletin of the Seismology Society, America* **84**, 972–1002.

Wilkerson, M. S., Medwedeff, D. A. and Marshak, S. (1991) Geometic modeling of fault-related folds: a pseudo-three-dimensional approach. *Journal of Structural Geology* **13**, 801–812.

Xiao, H. and Suppe, J. (1992) Origin of rollover. *Bulletin of the American Association of Petroleum Geologists* **76**, 509–529.

Yielding, G., Jackson, J. A., King, G. C. P., Sinval, H., Vita-Finzi, C. and Wood, R. M. (1981) Relations between surface deformation, fault geometry, seismicity and rupture characteristics during the El Asnam (Algeria) earthquake of 10 October, 1980. *Earth and Planetary Science Letters* **56**, 287–304.

Zepeda, R. L., Keller, E. A., Rockwell, T. K. and Ku, T. (1996) Active tectonics and soil chronology of Wheeler Ridge, Southern San Joaquin Valley, California. *Bulletin of the Geological Society, America*